Cable Function Analysis for the Musculoskeletal Static Workspace of a Human Shoulder

Article · August 2015

DOI: 10.1007/978-3-319-09489-2_19

4 authors:

Darwin Lau
The Chinese University of Hong Kong

Jonathan Eden
University of Melbourne

Saman K Halgamuge
Australian National University

Denny Oetomo
University of Melbourne

Cable Function Analysis for the Musculoskeletal Static Workspace of a Human Shoulder

Darwin Lau and Jonathan Eden and Saman K. Halgamuge and Denny Oetomo

Abstract The study of *cable function* allows the contribution of particular cables towards the generation of motion to be determined for cable-driven parallel manipulators (*CDPMs*). This study is fundamental in the understanding of the arrangement of cables for CDPMs and can be used within the design of optimal cable arrangements. In this paper, the analysis of cable function for the musculoskeletal static workspace of a human shoulder is performed. Considering the muscles within the shoulder as state dependent force generators, the set of muscles required in sustaining the gravity force is determined for each workspace pose. As a result, the set of poses that each muscle is responsible for (*muscle function*) can be computationally determined. By comparing the results to the muscle function from biomechanics studies, it is shown that the results from the proposed cable function analysis are consistent with that reported in the literature of human studies.

1 Introduction

Cable-driven parallel manipulators (*CDPMs*) have been widely studied in recent years due to their distinctive advantages: reduced end-effector weight and inertia compared to serial and traditional parallel rigid link mechanisms [1], potentially large reachable workspace [2] and high reconfigurability [3]. Moreover, CDPMs have been studied as bio-inspired systems [4, 5, 6] due to their anthropomorphic nature. Cables and rigid links of multilink cable-driven manipulators (*MCDMs*) can be regarded as structurally analogous to the muscles and bones of musculoskeletal systems, respectively. Furthermore, both cables and muscles can only provide unilateral actuation (*positive cable force*).

Darwin Lau, Jonathan Eden, Saman K. Halgamuge and Denny Oetomo
Department of Mechanical Engineering, University of Melbourne, Victoria 3010 Australia
e-mail: laudt@unimelb.edu, j.eden2@student.unimelb.edu.au, saman@unimelb.edu.au, doetomo@unimelb.edu.au

Workspace analysis has been widely studied on CDPMs to provide the operational region for a particular arrangement of cables [7, 8, 9, 10]. This can also be applied to musculoskeletal systems, however, the difference in the actuation dynamics between the cables and muscles must be considered. In [11], the impact of considering the *state-dependent force generator* property in physiological muscles on the static workspace of the human shoulder was studied. By comparing the static workspace with that generated using the *ideal force generator* cable model, it was observed that the state dependent active and passive muscle characteristics of a physiological muscle significantly impacted the static workspace. The musculoskeletal static workspace was compared to the range of motion reported by human benchmarks, and it was shown that the inclusion of the physiological muscle model resulted in a workspace more realistic to that of a human shoulder.

Workspace analysis is one approach that allows the impact of different arrangements in cable attachment locations to be observed [3, 12]. However, these approaches require that the workspace has to be regenerated each time in order to study the impact of different cable arrangements. As a result, the determination of the contribution of individual cables to the workspace is computationally expensive and has not been investigated in previous CDPM studies. The role of individual cables in generating motion or workspace (*cable function*) is beneficial in understanding the design of cable arrangement for a CDPM. This could be used in the optimisation of the attachment locations of the cables in a CDPM. For musculoskeletal systems, the study of *muscle function* can be used in a range of applications in rehabilitation robotics and biomechanics. For example, in the treatment of upper limb poststroke rehabilitation, the knowledge of muscle function would allow diagnosis of impairment and eventually lead to a more targeted rehabilitation treatment.

In biomechanics, muscle function has been studied for a range of human movements, such as the walking and running patterns of the gait [13], or in the motion of the shoulder [14, 15, 16, 17, 18]. In these studies, muscle function was determined by performing inverse dynamics on different trajectory motions. The limitations of this approach include: the determined muscle function results are limited to the selected trajectory, and the accuracy of the results is dependent on the choice of objective function used to resolve the muscle actuation redundancy.

In this paper, the analysis of muscle function to the musculoskeletal static workspace of the human shoulder is performed. The set of muscles that contribute to a particular static workspace pose can be generated by computing the maximum mass that the shoulder can withstand in that pose. This can be determined by computing the intersection of the ray of the gravity wrench vector and the surface of the wrench zonotype. The proposed approach allows the cable function for any state dependent force generator of CDPMs to be determined. By studying the muscle function of the human shoulder, it is shown that the results obtained are consistent with that reported in the literature of human studies. Compared with studying the muscle function for a specific trajectory, the proposed method allows the muscle function for the entire workspace to be determined without the need to solve for the inverse dynamics.

The remainder of the paper is organised as follows: Section 2 describes the analysis of the workspace of the human shoulder. Section 3 proposes the method to determine the cable function for any particular pose within the static workspace. Section 4 presents the study of muscle function over the static workspace of the human shoulder. Section 5 concludes the paper and presents areas of future work.

2 Musculoskeletal Static Workspace of the Human Shoulder

In this section, the physiological muscle model used in the cable function analysis and the generation of the musculoskeletal static workspace for the human shoulder are presented.

2.1 Hill-type Muscle Model

One widely accepted model of the physiological muscle is the *modified Hill-type model* [19] consisting of tendon and muscle elements connected in series. The combined muscle-tendon length l^{mt} can be expressed with respect to the tendon length l^t and the muscle length l^m. The relationship between the force that can be produced and the muscle-tendon length can be described by a set of generic force relationships and muscle specific properties [20]: peak isometric muscle force F_0^m, optimal muscle fibre length l_0^m, optimal muscle fibre pennation angle α_0 and tendon slack length l_s^t.

The tendon behaves as a passive non-linear elastic element. One model for the generic tendon force-strain relationship [20] can be analytically expressed as

$$\hat{F}^t(\varepsilon) = \begin{cases} 0 & \varepsilon < 0 \\ 0.10377\left(e^{91\varepsilon} - 1\right) & 0 \le \varepsilon < 0.01516 \\ 37.526\varepsilon - 0.26029 & 0.01516 \le \varepsilon < 0.1 \end{cases}, \tag{1}$$

where $\hat{F}^t$ and ε are the normalised tendon force and tendon strain, respectively. Tendon strain is defined by $\varepsilon = (l^t - l_s^t)/l_s^t$ and normalised tendon force is $\hat{F}^t = F^t/F_0^m$. The normalised muscle force $\hat{F}^m = F^m/F_0^m$ can be expressed as

$$\hat{F}^m(\eta) = \hat{F}_a^m(\eta)a(t) + \hat{F}_p^m(\eta), \tag{2}$$

where $\eta = l^m/l_0^m$ is the normalised muscle length and $0 \le a(t) \le 1$ is the activation level of the muscle at time t. The active muscle force $\hat{F}_a^m(\eta)$ relationship [20] and passive muscle force $\hat{F}_p^m(\eta)$ relationship [21] can be expressed as

$$\hat{F}_a^m(\eta) = \begin{cases} 1 - \left(\frac{\eta-1}{0.5}\right)^2 & 0.5 < \eta < 1.5 \\ 0 & \text{otherwise} \end{cases} \tag{3}$$

$$\hat{F}_p^m(\eta) = \eta^3 e^{8\eta - 12.9} . \tag{4}$$

In [11], it was shown that in static equilibrium the forces that can be produced by the muscle-tendon complex can be determined at any pose. Figure 1 shows the solution muscle-tendon forces for various muscle-tendon lengths l^{mt}. Curves F_1^t and F_5^t represent scenarios when the muscle is passive, with muscle-tendon forces of $F_1^{mt} = 0$ and F_5^{mt}, respectively. For curve F_3^t, the muscle-tendon complex is active and can have a range of muscle force $F^{mt} \in [F_{min}^{mt}, F_{max}^{mt}]$. The bold lines F_2^t and F_4^t represent the minimum and maximum muscle-tendon lengths for which the muscle is active, respectively.

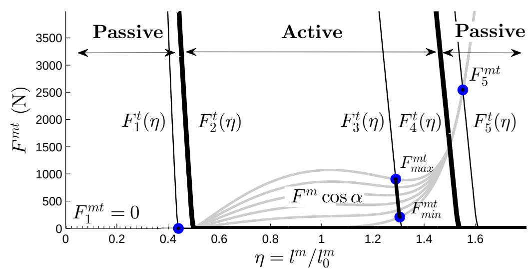

Fig. 1 Muscle-tendon forces for a range of l^{mt}, showing the scenarios in which the muscle is active and passive.

2.2 Shoulder Workspace

Using the Hill-type muscle model presented in Section 2.1 as a state dependent force generator, the static workspace for the human shoulder was studied [11]. As shown in Figure 2(a), the human shoulder consists of the *humerus* bone (end-effector) that is connected to the *scapular-clavicle* bone (base) through the *glenohumeral* joint. Accurate kinematics of the human shoulder were obtained from the well accepted OpenSim shoulder model developed by Holzbaur *et al.* [22], as shown in Figure 2(b). OpenSim is a widely accepted simulation platform in the biomechanics community used in performing analysis on musculoskeletal systems [23], for example, to study the muscle lengths and forces for a particular trajectory of motion.

The *glenohumeral* joint possesses three degrees-of-freedom and the pose of the system can be represented by $\mathbf{q} = \begin{bmatrix} \alpha & \beta & \gamma \end{bmatrix}^T$, where α, β, and γ are the *xyz*-Euler angles of the *glenohumeral* joint. Figure 2(a) shows the physiological interpretations for rotations in α, β and γ.

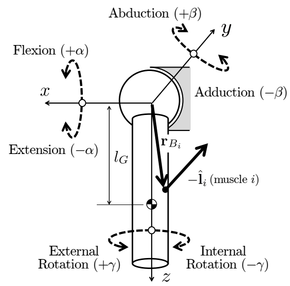

(a) Shoulder model kinematics

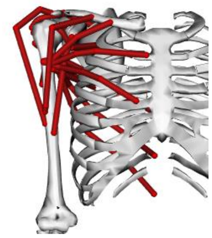

(b) OpenSim model

Fig. 2 Shoulder model consisting of the humerus bone and the glenohumeral joint. The rotations α, β and γ in (a) represent pure rotations about the x, y and z axes, respectively. The muscle geometry shown in (b) were obtained from the OpenSim shoulder model [22].

The mass, inertia and location of the centre of gravity for the average human *humerus* were obtained from [24]. The muscles for the shoulder model consists of $m = 15$ muscle sections that are identified as the main contributors to shoulder motion [22]: *deltoid* (*anterior, middle, posterior*), *supraspinatus, infraspinatus, subscapularis, teres minor, teres major, pectoralis major* (*clavicular, sternal, ribs*), *latissimus dorsi* (*thoracic, lumbar, iliac*) and *coracobrachialis*. The muscle properties F_0^m, l_0^m, l_s^t and α_0 for each muscle sub-region were obtained from [22]. For the shoulder system, the transpose of the Jacobian matrix can be expressed as

$$L^T = \left[\, \mathbf{r}_{B_1} \times \hat{\mathbf{l}}_1 \;\; \mathbf{r}_{B_2} \times \hat{\mathbf{l}}_2 \;\ldots\; \mathbf{r}_{B_{15}} \times \hat{\mathbf{l}}_{15} \,\right]. \tag{5}$$

As shown in Figure 2(a), the vectors $\mathbf{r}_{B_i}$ and $\hat{\mathbf{l}}_i$ represent the insertion location to the humerus and the direction vector of the insertion, respectively, for muscle i. The equations of motion for the system can be represented as

$$M(\mathbf{q})\ddot{\mathbf{q}} + \mathbf{C}(\dot{\mathbf{q}}, \mathbf{q}) + \mathbf{G}(\mathbf{q}) = -L(\mathbf{q})^T \mathbf{f}, \tag{6}$$

where M, $\mathbf{C}$, $\mathbf{G}$ correspond to the mass inertia matrix, centrifugal and Coriolis force vector, and gravitational vector, respectively. The musculoskeletal static workspace can be defined as

$$SW^* = \left\{ \mathbf{q} : \mathbf{G}(\mathbf{q}) + L_p^T \mathbf{f}_p = -L_a^T \mathbf{f}_a, \exists \mathbf{f}_a \in [\, \underline{\mathbf{f}_a}, \overline{\mathbf{f}_a}] \right\}. \tag{7}$$

The vector $\mathbf{f}_p$ and matrix L_p^T represent passive muscle forces and the transpose of the passive muscle Jacobian matrix, respectively. Similarly, the vector $\mathbf{f}_a$ and matrix L_a^T represent the active muscle forces and transpose of the active muscle Jacobian matrix, respectively. The passive muscle forces $\mathbf{f}_p$ and active muscle force ranges

$\mathbf{f}_a \in [\underline{\mathbf{f}_a}, \overline{\mathbf{f}_a}]$ can be solved using the approach presented in [11]. Figure 3 shows the musculoskeletal static workspace defined by (7) for the human shoulder [11].

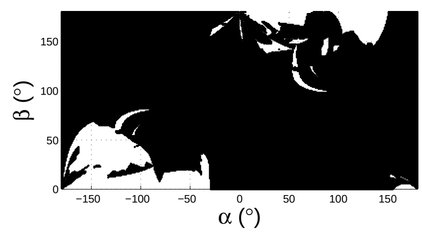

Fig. 3 The α-β cross section of the musculoskeletal static workspace for the human shoulder for zero rotation ($\gamma = 0°$)

3 Gravity Force Cable Function at a Pose

One approach to study the cable function of a musculoskeletal system is to consider the set of cables required in generating the maximum weight that the system can sustain. First, consider the set of wrenches $\mathscr{W}_{avail}(\mathbf{q})$ that can be produced by a state dependent force generator at a given pose as

$$\mathscr{W}_{avail}(\mathbf{q}) = \left\{\mathbf{w} : \mathbf{w} = -L^T(\mathbf{q})\mathbf{f},\ \forall \mathbf{f} \in [\underline{\mathbf{f}}, \bar{\mathbf{f}}]\right\} , \tag{8}$$

where $\underline{\mathbf{f}}$ and $\bar{\mathbf{f}}$ represent the minimum and maximum forces that the system can generate at pose $\mathbf{q}$, respectively.

At each pose, the available wrench set $\mathscr{W}_{avail}(\mathbf{q})$ in (8) can be generated through the convex hull method presented in [7]. In this method, the zonotope wrench set $\mathscr{W}_{avail}(q)$ is constructed using the convex hull of a set defined as

$$H = \left\{ \mathbf{w} \in \mathbb{R}^n | \mathbf{w} = \sum_{i=1}^{m} f_i \mathbf{l}_i,\ f_i \in \left\{\underline{f_i}, \overline{f_i}\right\} \right\}, \tag{9}$$

where n is the number of degrees-of-freedom and m is the number of cables. The maximum and minimum mass for cable i is represented by $\underline{f_i}$ and $\overline{f_i}$, respectively. The vector $\mathbf{l}_i$ corresponds to the i-th column of the matrix $-L^T(\mathbf{q})$. The convex hull is constructed from the set of 2^m vertices representing the combinations of the minimum and maximum cable forces of the system. For highly redundant systems, a large number of these vertices may be located inside the generated convex hull.

Each vertex represents a combination of a set of minimum and maximum cable forces (9).

If a pose is within the static workspace, then the gravity wrench $\mathbf{G}(\mathbf{q})$ is within the available wrench set $\mathscr{W}_{avail}(\mathbf{q})$. If the mass of the system is denoted as m_s, then the normalised gravity wrench can be defined as $\hat{\mathbf{G}}(\mathbf{q}) = \mathbf{G}(\mathbf{q})/m_s$. Allowing the mass of the system to vary, the vector $\Gamma(\mathbf{q}) = m\hat{\mathbf{G}}(\mathbf{q})$ is geometrically equivalent to a ray in $\mathbb{R}^n$. For each pose that is within the static workspace, there exists a section of the ray that lies within the available wrench set $\Gamma(\mathbf{q}) \subset \mathscr{W}_{avail}(\mathbf{q})$ defined by

$$\Gamma(\mathbf{q}) = \{m\hat{\mathbf{G}}(\mathbf{q}),\ m \in [m_{min}, m_{max}]\}. \tag{10}$$

The minimum mass $m_{min} \geq 0$ and maximum mass $m_{max} > 0$ can be determined by solving for the intersections between the ray $\Gamma(\mathbf{q})$ and the surfaces of $\mathscr{W}_{avail}(\mathbf{q})$.

The surfaces of $\mathscr{W}_{avail}(\mathbf{q})$ represent the minimum and maximum wrenches that could be produced by the vertices from (9). Each of the surfaces V_k can be defined by the parametric relationship

$$V_k = \mathbf{v_0} + s(\mathbf{v_1} - \mathbf{v_0}) + t(\mathbf{v_2} - \mathbf{v_0}), \tag{11}$$

where $\mathbf{v_0}, \mathbf{v_1}$ and $\mathbf{v_2}$ represent the vertices within $\mathscr{W}_{avail}(\mathbf{q})$ that define the surface V_k. Each of the vertices $\mathbf{v_0}, \mathbf{v_1}$ and $\mathbf{v_2}$ from (11) corresponds to a set of active muscles at maximum activation to form the vertex and can be defined as $\mathscr{M}_{v_0}(\mathbf{q})$, $\mathscr{M}_{v_1}(\mathbf{q})$ and $\mathscr{M}_{v_2}(\mathbf{q})$, respectively.

An intersection between the ray (10) and surface V_k from (11) exists if a solution to $\Gamma(\mathbf{q}) = V_k$ can be found under the constraints

$$m \geq 0,\ s \geq 0,\ t \geq 0,\ s + t \leq 1\ . \tag{12}$$

As a result, the set of muscles $\mathscr{M}(\mathbf{q})$ contribute to producing the maximum gravity wrench can be determined by

$$\mathscr{M}(\mathbf{q}) = \mathscr{M}_{v_0}(\mathbf{q}) \cup \mathscr{M}_{v_1}(\mathbf{q}) \cup \mathscr{M}_{v_2}(\mathbf{q}). \tag{13}$$

To illustrate the wrench set and the determination of the set of contributing muscles (*muscle function*), consider the example of the human shoulder system presented in Section 2.2 at the pose $\mathbf{q}_{abduction} = [\alpha\ \beta\ \gamma]^T = [0°\ 60°\ 0°]^T$. Figure 4(a) shows the forces that each muscle is capable of producing at pose $\mathbf{q}_{abduction}$.

Figure 4(b) shows the resulting wrench set $\mathscr{W}_{avail}(\mathbf{q}_{abduction})$ for the shoulder system at pose $\mathbf{q}_{abduction}$. The intersection between the ray $\Gamma(\mathbf{q}_{abduction})$ and the wrench set is also shown in the figure. In this example, the ray and wrench set intersected at $m = m_{max} = 39.11$ kg and the set of muscles that contribute to the intersecting surface is $\mathscr{M}(\mathbf{q}_{abduction}) = \{3, 4, 5, 6, 7, 12, 13, 14\}$. Furthermore, from Figure 4(a) it can be observed that within $\mathscr{M}(\mathbf{q}_{abduction})$ muscles number 3, 5 and 12 have the largest capability in producing the gravity wrench. In addition to producing the maximum gravity wrench, the muscles were also required to counteract the passive muscle force of muscle number 2. From the example, by observing set of muscles

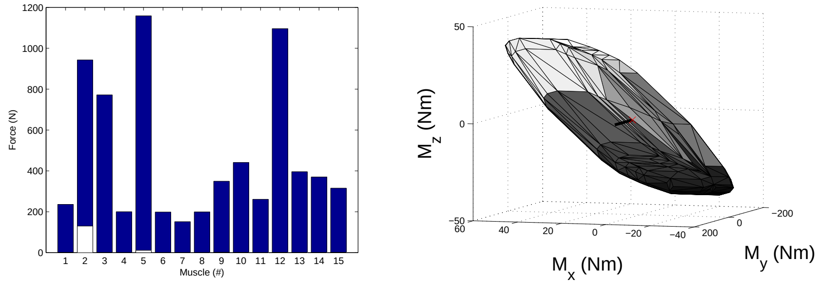

(a) Muscle force ranges (b) Resultant wrench set

Fig. 4 The muscle wrench set $\mathscr{W}_{avail}(\mathbf{q}_{abduction})$ for the human shoulder at pose $\mathbf{q}_{abduction} = [0^\circ\ 60^\circ\ 0^\circ]^T$ showing the solution to the muscle function for the gravity wrench. The solid bars in (a) represent the range of force that can be produced by the muscles in pose $\mathscr{W}_{avail}(\mathbf{q}_{abduction})$.

required in generating the maximum force in a particular direction of force (the gravity wrench $\hat{\mathbf{G}}$ in this study), the function of muscles can be determined.

4 Muscle Function over the Workspace

In Section 3, the method to determine the set of muscles required to sustain the gravity wrench was shown. By analysing the contribution of muscles for every pose, the muscle function for the static workspace can be studied. In this section, the function for different muscles on the workspace is analysed and compared to that from biomechanics studies. Figure 5 shows the poses that each muscle contributes to the maximum gravity wrench. From the muscle function cross-sections, it can be observed that different muscles contribute to gravity wrench in different poses within the static workspace.

It can be observed that the set of deltoid muscles (Figure 5(a), 5(b) and 5(c)) is a contributor to shoulder flexion (positive α direction and zero β), extension (negative α direction and zero β) and abduction (positive β direction and zero α) [14, 15, 16]. Furthermore, this is consistent with the literature that the deltoid anterior, deltoid middle and deltoid posterior muscle sections are primarily responsible for shoulder flexion, abduction and extension, respectively.

Furthermore, it can be observed that the set of pectorialis muscles (Figure 5(d), 5(e) and 5(f)) is predominantly responsible for flexion motion [17]. Additionally, it can be observed that the three subregions of the pectorialis muscle perform a very similar muscle function. This is consistent with the fact that the three muscle subregions are arranged at similar locations on the shoulder [22].

Similarly, Figures 5(g), 5(h) and 5(i) show that the three subregions of the latissimi dorsi have a similar muscle function, and is known to be largely responsible for the extension motion of the shoulder [18]. Additionally, it can be observed that the

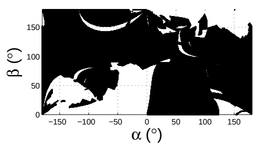

(a) Deltoid (anterior)

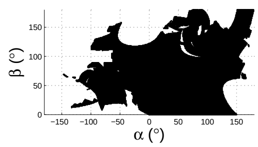

(b) Deltoid (middle)

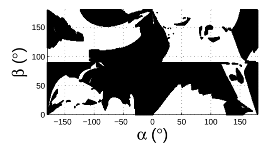

(c) Deltoid (posterior)

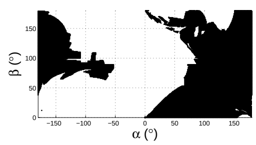

(d) Pectorialis (sternal)

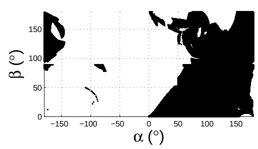

(e) Pectorialis (clavicular)

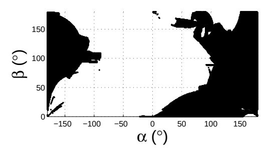

(f) Pectorialis (Ribs)

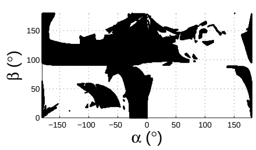

(g) Latissimi dorsi (thoracic)

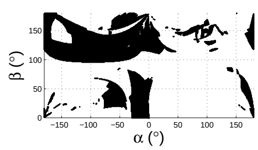

(h) Latissimi dorsi (lumbar)

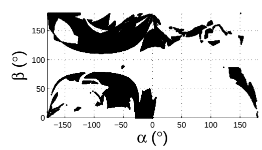

(i) Latissimi dorsi (iliac)

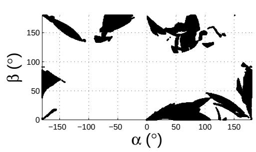

(j) Coracobrachialis

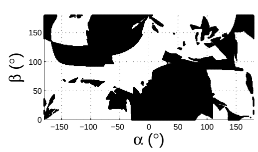

(k) Infraspinatus

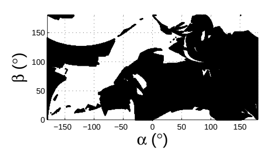

(l) Subscapularis

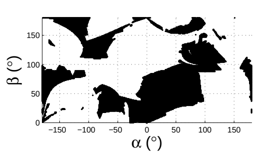

(m) Supraspinatus

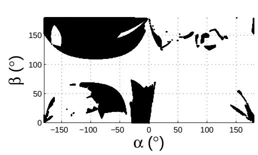

(n) Teres major

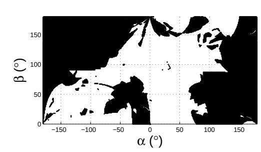

(o) Teres minor

Fig. 5 Muscle function for the set of muscles in the human shoulder on the α-β cross section for zero rotation ($\gamma = 0°$). The shaded region corresponds to the poses in which the particular muscle is required to sustain the maximum gravity force.

latissimi dorsi muscles only contribute to small degrees of abduction. This result is also consistent with the literature where it has been observed that the strength of the muscles diminishes as the amount of abduction is increased. This indicates that the muscle force range and corresponding affect on the wrench polygon also diminishes with increasing abduction. The functions of muscles in Figures 5(j) to 5(o) can be interpreted in the same manner.

Compared with previous biomechanics studies, the proposed approach provides a more complete description of muscle function over the entire workspace, not requiring any trajectory or inverse dynamics objective function to be specified. The muscle functions obtained represent the muscles that are responsible for producing the largest force in a particular direction, for example, the gravity wrench. In addition the function of each muscle, Figure 6 shows the maximum mass that can be sustained for the gravity force over the α-β workspace cross-section for zero rotation $\gamma = 0°$.

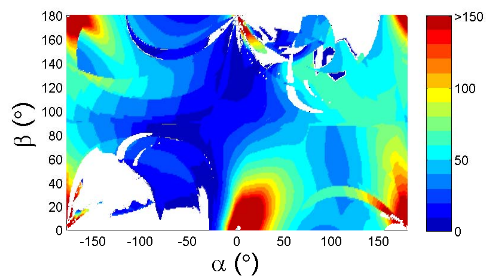

Fig. 6 The maximum mass that the shoulder muscles can sustain on the α-β cross section for zero rotation ($\gamma = 0°$).

It can be observed from Figure 6 that the shoulder is capable of sustaining gravity forces from masses of few kilograms to above 150 kg. The capability of the shoulder to sustain mass is dependent on the shoulder pose as the moment arms vary for both the gravity force and the set of muscles. This approach in studying muscle function allows the capabilities of the shoulder to be studied for varying properties and attachment locations of the muscles.

In addition to the distribution of mass that can be obtained from the approach, the number of muscles required in producing the maximum mass is also beneficial in the study of a CDPM. Figure 7 shows the dimension of $\mathscr{M}(\mathbf{q})$, or the number of muscles required to generate the maximum mass, for the different poses within the workspace. It can be observed that for a majority of the α-β workspace cross-section, an average of 6 to 9 cables were required to produce the maximum gravity wrench. This describes the level of redundancy in generating the gravity wrench ray $\Gamma(\mathbf{q})$. Hence, for masses $m < m_{max}$, a subset of the muscles could be selected to counteract the gravity force.

It should be noted that in the proposed approach, the resulting muscle function shown is limited to one particular direction of force, the gravity force in this study.

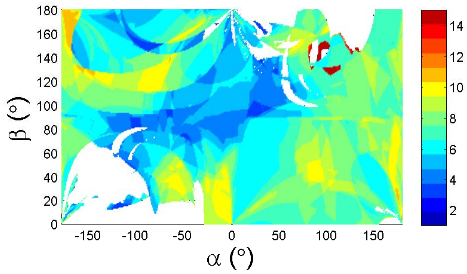

Fig. 7 The number of muscles required in sustaining the maximum mass on the α-β cross section for zero rotation ($\gamma = 0°$).

However, the selection of the gravity wrench is a natural choice in studying the function of the human shoulder. For example, many common actions performed by the upper arm is in the direction opposite to gravity, such as the swinging of the arm, to lift heavy objects or in exercises for the upper limb.

5 Conclusion

The analysis of cable function on the musculoskeletal static workspace of the human shoulder was performed. It was shown that the cable function for state dependent force generators could be determined by computing the set of cables required in balancing the maximum gravity force. The function of muscles for the human shoulder was performed to demonstrate the proposed method. The results were compared to the muscle function obtained from motion analysis performed in biomechanics studies, showing that the obtained results matched that from human studies. The proposed method provides a more complete description of muscle function than that of trajectory based approaches. Future work will focus on studying the muscle function for changes in actuator properties and different pathological conditions.

References

1. J. S. Albus, R. V. Bostelman, and N. Dagalakis, "The NIST robocrane," *J. Robot. Syst.*, vol. 10, no. 5, pp. 709–724, 1993.
2. R. L. Williams II, J. S. Albus, and R. V. Bostelman, "3D cable-based cartesian metrology system," *J. Robot. Syst.*, vol. 21, no. 5, pp. 237–257, 2004.
3. D. Lau, K. Bhalerao, D. Oetomo, and S. K. Halgamuge, "On the task specific evaluation and optimisation of cable-driven manipulators," in *Advances in Reconfigurable Mechanisms and Robots I*, J. S. Dai, M. Zoppi, and X. Kong, Eds. Springer London, 2012, ch. 63, pp. 707–716.
4. D. Lau, D. Oetomo, and S. K. Halgamuge, "Generalized modeling of multilink cable-driven manipulators with arbitrary routing using the cable-routing matrix," *IEEE Trans. Robot.*, vol. 29, no. 5, pp. 1102–1113, 2013.

5. T. Kozuki, H. Mizoguchi, Y. Asano, M. Osada, T. Shirai, J. Urata, Y. Nakanishi, K. Okada, and M. Inaba, "Design methodology for thorax and shoulder of human mimetic musculoskeletal humanoid kenshiro - a thorax with rib like surface -," in *Proc. IEEE/RSJ Int. Conf. Intell. Robot. Syst.*, 2012, pp. 3687–3692.
6. S. Wittmeier, C. Alessandro, N. Bascarevic, K. Dalamagkidis, D. Devereux, A. Diamond, M. Jäntsch, K. Jovanovic, R. Knight, H. G. Marques, P. Milosavljevic, B. Mitra, B. Svetozarevic, V. Potkonjak, R. Pfeifer, A. Knoll, and O. Holland, "Toward anthropomimetic robotics: Development, simulation, and control of a musculoskeletal torso," *J. Artif. Life*, vol. 19, no. 1, pp. 171–193, 2013.
7. S. Bouchard, C. Gosselin, and B. Moore, "On the ability of a cable-driven robot to generate a prescribed set of wrenches," *J. Mech. Robot.*, vol. 2, no. 1, pp. 011 010/1–10, 2010.
8. W. B. Lim, G. Yang, S. H. Yeo, and S. K. Mustafa, "A generic force-closure analysis algorithm for cable-driven parallel manipulators," *Mech. Mach. Theory*, vol. 46, no. 9, pp. 1265–1275, 2011.
9. D. Lau, D. Oetomo, and S. K. Halgamuge, "Wrench-closure workspace generation for cable driven parallel manipulators using a hybrid analytical-numerical approach," *J. Mech. Des.*, vol. 133, no. 7, pp. 071 004/1–7, 2011.
10. M. Gouttefarde, D. Daney, and J.-P. Merlet, "Interval-analysis-based determination of the wrench-feasible workspace of parallel cable-driven robots," *IEEE Trans. Robot.*, vol. 27, no. 1, pp. 1–13, 2011.
11. D. Lau, J. Eden, D. Oetomo, and S. K. Halgamuge, "Musculoskeletal static workspace of the human shoulder as a cable-driven robot," *IEEE/ASME Trans. Mechatron.*, vol. 99, no. 0, pp. 1–6, 2014.
12. X. Tang, L. Tang, J. Wang, and D. Sun, "Workspace quality analysis and application for a completely restrained 3-dof planar cable-driven parallel manipulator," *J. Mech. Sci. Technol.*, vol. 27, no. 8, pp. 2391–2399, 2013.
13. K. Sasaki and R. R. Neptune, "Differences in muscle function during walking and running at the same speed," *J. Biomech.*, vol. 39, no. 11, pp. 2005–2013, 2006.
14. J. A. Ringelberg, "EMG and force production of some human shoulder muscles during isometric abduction," *J. Biomech.*, vol. 18, no. 12, pp. 939–947, 1985.
15. M. Kronberg and L.-A. Brostrom, "Electromyographic recordings in shoulder muscles during eccentric movements," *Clin. Orthop. Relat. R.*, vol. 314, pp. 143–151, 1995.
16. R. F. Escamilla, K. Yamashiro, L. Paulos, and J. R. Andrews, "Shoulder muscle activity and function in common shoulder rehabilitation exercises," *Sports Med.*, vol. 39, no. 8, pp. 663–685, 2009.
17. N. Palastanga, D. Field, and R. W. Soames, *Anatomy and Human Movement: Structure and Function*, 5th ed. Edinburgh: Butterworth-Heinemann Elsevier, 2006.
18. M. E. Gerling and S. H. Brown, "Architectural analysis and predicted functional capability of the human latissimus dorsi muscle," *J. Anat.*, vol. 223, no. 2, pp. 112–122, 2013.
19. F. E. Zajac, "Muscle and tendon: Properties, models, scaling, and application to biomechanics and motor control," *Crit. Rev. in Biomed. Eng.*, vol. 17, no. 4, pp. 359–411, 1989.
20. C. F. Martin and L. Schovanec, "The control and mechanics of human movement systems," *Progress in Systems and Control Theory*, vol. 25, pp. 173–202, 1999.
21. M. Vilimek, "Musculotendon forces derived by different muscle models," *Acta of Bioeng. and Biomech.*, vol. 9, no. 2, pp. 41–47, 2007.
22. K. R. S. Holzbaur, W. M. Murray, and S. L. Delp, "A model of the upper extremity for simulating musculoskeletal surgery and analyzing neuromuscular control," *Ann. Biomed. Eng.*, vol. 33, no. 6, pp. 829–840, 2005.
23. S. L. Delp, F. C. Anderson, A. S. Arnold, P. Loan, A. Habib, C. T. John, E. Guendelman, and D. G. Thelen, "OpenSim: Open-source software to create and analyze dynamic simulations of movement," *IEEE Trans. Biomed. Eng.*, vol. 54, no. 11, pp. 1940–1950, 2007.
24. J. Yu, D. C. Ackland, and M. G. Pandy, "Shoulder muscle function depends on elbow joint position: An illustration of dynamic coupling in the upper limb," *J. Biomech.*, vol. 44, no. 10, pp. 1859–1868, 2011.